

Adenylate Cyclase 7 Is Implicated in the Biology of Depression and Modulation of Affective Neural Circuitry

Supplement 1

SERT^{KO} Behavioral Phenotype is Consistent with a Robust Anxious Depressive-Like Syndrome

-- The behavioral results include prior and new data, and essentially confirm prior reports on SERT^{KO} mice. Accordingly, this section is presented in the supplement only.

Results

Major depression is defined as a syndrome (i.e. collection of symptoms) including low mood or anhedonia, accompanied by cognitive (e.g. attention, concentration) and physiological symptoms (e.g. weight, locomotor and sleep pattern changes), and frequently co-morbid with significant anxiety symptoms. Thus, its emotionality component is best characterized in mice by a comprehensive panel of behavioral tests for anxiety-like and depressive-like emotionality, and for antidepressant-like behavior. SERT^{KO} display robust anxiety-like behaviors in the open field and elevated plus maze tests (1-3) (Figure S1A-C; adapted from 3-month baseline results in (4)). SERT^{KO} also display increased latency to feed in the novelty-suppressed feeding (NSF) test (Figure S1D) (2,5), a behavior associated with elevated anxiety-like and depressive-like emotionality (6). Here we also show that SERT^{KO} mice display a significant decreased preference for sucrose consumption (Figure S1E,F), typically interpreted as a rodent homolog to an anhedonia-like state. Finally, under our experimental conditions, SERT^{KO} mice did not display behaviors that could be interpreted as predictive of antidepressant effect in the forced swim test and tail suspension tests (Figure S1G,H). Summarizing current and prior characterization, SERT^{KO} mice demonstrate a robust phenotype indicative of an anxious depressive-like syndrome.

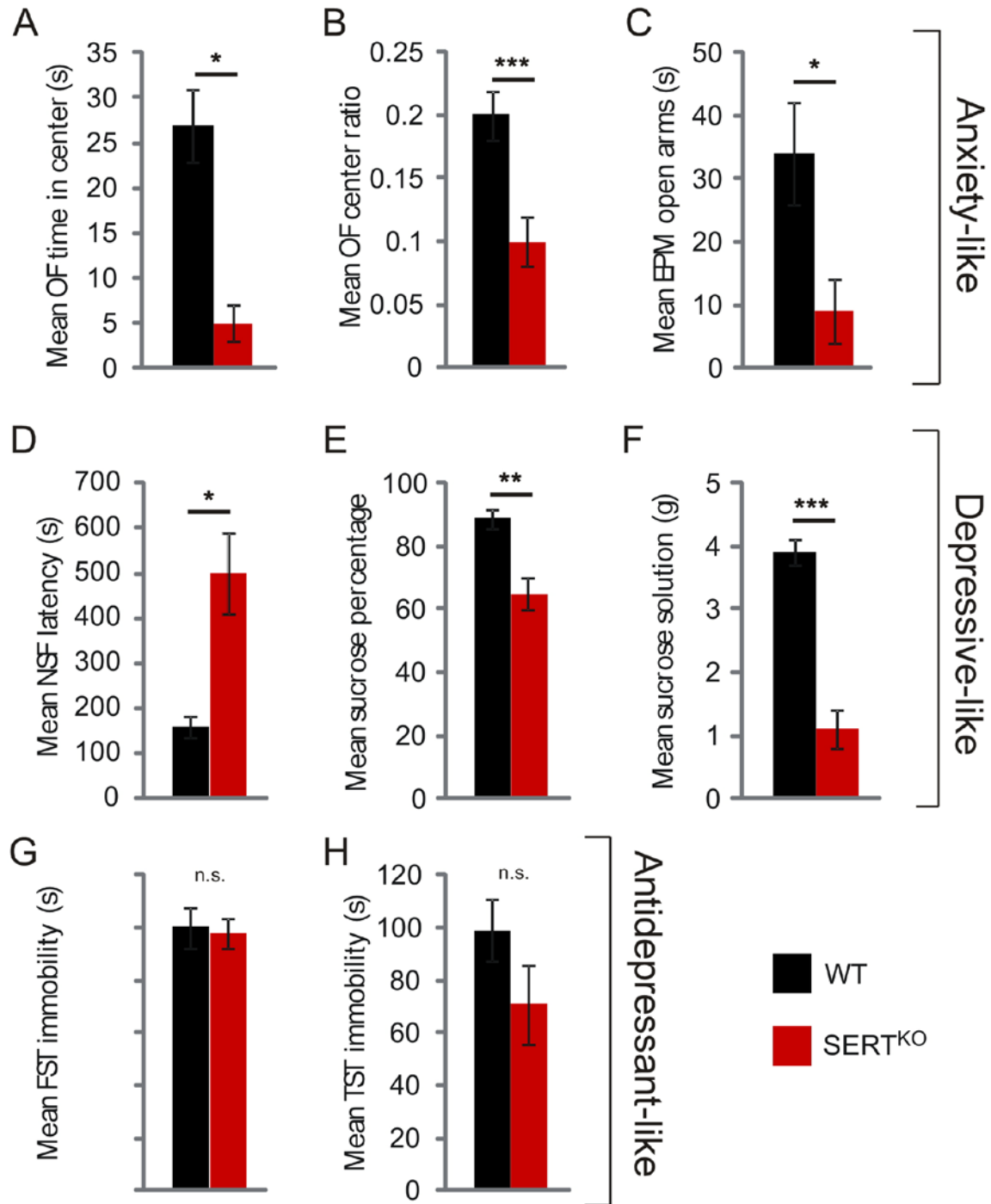


Figure S1. Anxious depressive-like syndrome in SERT^{KO} mice. (A to C) The decreased activity in the threatening open compartment of the open field (OF) and in the open arms of the elevated plus maze (EPM) confirm the previously reported increased anxiety-like behavior in

SERT^{KO}. OF (Time in center): WT, $n = 19$, SERT^{KO}, $n = 18$, $p = 0.002$; OF (center ratio): wild-type (WT), $n = 19$, SERT^{KO}, $n = 17$, $p = 0.0007$; EPM (time in open arms): WT, $n = 19$, SERT^{KO}, $n = 19$, $p = 0.032$. (D to F) Increased depressive-like behaviors of SERT^{KO} mice are demonstrated by the increased latency to feed in the threatening environment of the novelty-suppressed feeding (NSF) test and by a significant decrease in sucrose consumption. NSF: WT, $n = 19$, SERT^{KO}, $n = 19$, $p = 0.02$. Sucrose preference test: WT, $n = 36$, SERT^{KO}, $n = 37$; percentage, $p = 0.003$; Total sucrose solution, $p = 4 \times 10^{-5}$. (G-H) SERT^{KO} mice display similar immobility time in the forced swim (FST) and tail suspension (TST) tests, indicating an absence of behavior predictive of antidepressant activity. FST: WT, $n = 19$, SERT^{KO}, $n = 19$, $p > 0.05$. TST: WT, $n = 18$, SERT^{KO}, $n = 18$, $p > 0.05$. * $p < .05$; ** $p < .005$; *** $p < .0005$; error bars represent standard error of the mean. Not shown: SERT^{KO} hypolocomotion was confirmed in OF and EPM (4); no differences in weight loss or home-cage feeding in NSF; no difference in water consumption in sucrose preference. Figures A-D were adapted from the 3-month baseline study in (4).

Material and Methods

Animals

SERT^{KO} and wild-type (WT) C57BL/J6 littermates (7) were obtained from Taconic (Hudson, New York) and bred via heterozygous breeding. Experimental cohorts were comprised of male WT and SERT^{KO} littermates. Cohort 1 included 36 WT and 37 SERT^{KO} mice at 3-6 months of age, which were tested in open field (OF), novelty-suppressed feeding (NSF), and sucrose preference (SP) in order to evaluate SERT^{KO} baseline behavior relative to WT. Cohort 2 included 19 WT and 19 SERT^{KO} mice at 3-6 months of age which were tested in elevated plus maze (EPM), forced swim test (FST), and tail suspension test (TST) (4). Cohort 3 included 5 WT and 5 SERT^{KO} mice at 3-5 months of age, from which amygdala and cingulate cortex tissue samples were collected for microarray analysis of gene expression. Cohort 4 included 10 WT and 10 SERT^{KO} mice at 3-5 months of age, from which amygdala and cingulate tissue samples

were collected for quantitative polymerase chain reaction (qPCR) validation of differential gene expression. Results from OF, EPM in cohort 1 and from NSF in cohort 2 were previously described (4). All mice were maintained on a 12-hour light cycle with access to food *ad libitum*, and all procedures received Institutional Animal Care and Use Committee (IACUC) approval.

Anxiety-like, Depressive-like and Antidepressant-like Behavioral Testing

OF. Time in center and activity in center (normalized to total activity) was measured relative to a 16 even-size squares grid on the floor of the 30 x 30 cm open field, as described (8). The total number of gridline crosses was used as an index of locomotor activity. Amount of time and gridline crosses within the squares of the aversive center were recorded for 10 minutes, and the ratio of crosses into the center compared to the total number of crosses was calculated to evaluate anxious emotionality.

EPM. Time in open arms and number of entries into open arms (normalized to total entries) was measured in EPM as described (8), using a cross maze with two open and two closed 30 x 5 cm arms. The total number of entries was used as a second index of locomotor activity. The ratio of entries and time spent in the open and closed arms was recorded for 10 minutes to evaluate anxious emotionality.

NSF. Mice were food deprived for 16 hours and then placed in a novel, empty and brightly-lit chamber with one food pellet placed in the center. In NSF, the latency to feed correlates with fearfulness and decreases after acute treatment with anxiolytic drugs (9) or chronic antidepressant exposure (6). The test was applied as described (6) with an increased session duration (30 min). During testing, a food pellet was placed in the brightly-lit center of the 30 x 60 cm chamber. A control measure of food consumption was monitored in the home cage after the test over the next 24 hours.

SP. After 24 hours of training to drink from customized tubes filled with sweetened condensed milk, mice were provided with identical tubes of 2% sucrose and water, and the consumption was measured by weight following a 16-hour period. The ratio of sucrose solution

to total volume consumed indicates a preference for sucrose solution when greater than 0.50, and mice with a ratio of sucrose solution consumption lower than control are thought to display anhedonia-like emotionality.

FST. Duration of immobility of the mouse was measured in a 3-liter beaker of water at room temperature in a 6-minute trial (2-minute intervals were measured). Because no changes over time were measured, the results are reported as a total duration of immobility out of a 6 minute trial.

TST. Duration of immobility was measured while each mouse was suspended by the tail in a 6-minute trial (2-minute intervals were measured). Because no changes over time were measured, the results are reported as a total duration of immobility out of a 6 minute trial.

Behavior Statistical Analysis was performed by two-group *t*-test to define the effect of genotype.

ADCY7 Immunoblotting

Protein Isolation

Acetone precipitation of proteins was carried out following the RNA extraction from the Trizol samples from amygdala region of brain tissues from control and major depressive disorder (MDD) subjects. The lower red phenol-chloroform phase was used for protein isolation, using ethanol to precipitate DNA, and acetone to extract protein from the supernatant. The supernatant was collected after 5 minute centrifugation at 14,000 rpm. Following extensive washes, the dried pellet was dissolved in 1x SDS buffer. An aliquot was used for protein quantification using Pierce BCA assay (Pierce, Rockford, IL). In order to detect the ADCY7 band, we loaded 5 to 40 ug of protein/well and resolved by SDS-PAGE in 10% Tris/glycine gels. The expected migration for ADCY7 is ~120 kD and for beta Actin is 37 kD. In addition, we

isolated protein samples from mouse lung, heart and brain to check for tissue specificity of ADCY7.

Western blot analysis was performed following SDS-PAGE using the Odyssey system (LI-COR Biosciences, Lincoln, NE) as described previously (10). In brief, gel-transferred polyvinylidene fluoride membrane were blocked in LI-COR blocking buffer and incubated with mouse anti-actin, at 0.5 ug/mL (Sigma #: A 2228, St. Louis, MO) and four different sources of primary antibodies for ADCY7 including 1) Rabbit polyclonal antibody (SC-25501, from Santa Cruz Biotechnology, Santa Cruz, CA), at 0.5 ug/mL concentration, 2) Rabbit polyclonal antibody (PA1-31193 from Thermo Scientific, Rockford, IL) at 1:250 concentration, 3) Rabbit polyclonal antibody (ab14782 Abcam, Cambridge, MA) at 1:500 and 4) Rabbit polyclonal antibody AC-7 (kindly provided by Dr. Boris Tabakoff, University of Colorado, Denver, CO) at 1:3000 concentration (11). Fluorescent IR Dye 680 anti-rabbit and fluorescent IR Dye 800 anti-mouse (LI-COR Biosciences) secondary antibodies were used in signal detection. The Li-Cor Odyssey Infrared imaging system captures the whole dynamic range of infrared fluorescence using small quantities of protein. Each primary antibody was incubated for a period of 14 hrs at 4°C. Samples were processed in matched pairs on the same gel.

We did not detect any positive signals by using the antibodies listed above. In mouse samples, we used increased protein loading 10 ug to 40 ug of protein per lane and with different antibody concentrations. None of the antibodies gave rise to the expected 120 kD band using protein isolated from human amygdala or from mouse (three different tissues). We did detect a ~200 kD band using the Thermo Scientific antibody, but in the absence of positive control (i.e. proper size band), it was unclear whether the observed ~200 kD band was non-specific or due to protein aggregation.

Imaging Genetics Methods

Participants

The two independent samples (Sample 1: $n = 82$, 46 women, mean age 44.76 ± 6.47 ; Sample 2: $n = 98$; 40 women, mean age 40.53 ± 7.93) were recruited from two consecutive stages of the larger Adult Health and Behavior (AHAB) Study, which investigates a variety of behavioral and biological traits among non-patient, middle-aged community volunteers. All participants included in our analyses were in good general health and free of the following: 1) medical diagnoses of cancer, stroke, diabetes requiring insulin treatment, chronic kidney or liver disease, or a lifetime history of psychotic symptoms; 2) use of psychotropic, glucocorticoid, or cardiovascular (e.g., antihypertensive or antiarrhythmic) medication; 3) conditions that affect cerebral blood flow and metabolism (e.g., hypertension); and 4) any current DSM-IV Axis I disorder as assessed by the nonpatient version of the Structured Clinical Interview for DSM-IV (12).

Amygdala Reactivity Paradigm

The experimental functional magnetic resonance imaging (fMRI) paradigm consisted of 4 blocks of a face-processing task interleaved with 5 blocks of a sensorimotor control task (13-15). Participant performance (accuracy and reaction time) was monitored during all scans. During the face-processing task, participants viewed a trio of faces (expressing either anger or fear) and selected 1 of 2 faces (bottom) that was identical to a target face (top). Angry and fearful facial expressions can represent honest indicators of an ecologically valid threat, especially that related to conspecific challengers (16). Within this context, we interpret the amygdala activation elicited by our task as being threat-related. Each face-processing block consisted of 6 images, balanced for sex and target affect (angry or fearful), all of which were derived from a standard set of pictures of facial affect (17). During the sensorimotor control blocks, participants viewed a trio of simple geometric shapes (circles and vertical and horizontal

ellipses) and selected 1 of 2 shapes (bottom) that were identical to a target shape (top). Each sensorimotor control block consisted of 6 different shape trios. All blocks were preceded by a brief instruction (“Match faces” or “Match shapes”) that lasted 2 seconds. In the face-processing blocks, each of the 6 face trios was presented for 4 seconds with a variable interstimulus interval of 2 to 6 seconds (mean, 4 seconds), for a total block length of 48 seconds. In the sensorimotor control blocks, each of the 6 shape trios was presented for 4 seconds with a fixed interstimulus interval of 2 seconds, for a total block length of 36 seconds. Total task time was 390 seconds. As we were not interested in neural networks associated with face-specific processing *per se*, but rather in eliciting a maximal amygdala response across all participants so we could then investigate for genotype effects, we chose not to use neutral faces as control stimuli because neutral faces can be subjectively experienced as affectively laden or ambiguous and thus engage the amygdala (18,19).

Blood Oxygen Level-Dependent (BOLD) fMRI Acquisition Parameters

Scans for Sample 1 were acquired on a Siemens 3T MAGNETOM Allegra platform while those for Sample 2 were acquired on Siemens 3T MAGNETOM Trio platform (Siemens AG, Erlangen, Germany). On each platform BOLD functional images were acquired with a gradient-echo echoplanar imaging sequence (TR = 2000 ms, TE = 25 ms, FOV = 20 cm, matrix 64 x 64), which covered 34 interleaved axial slices (3-mm slice thickness) aligned with the anterior and posterior commissure plane and encompassing the entire cerebrum and most of the cerebellum. Before collecting fMRI data for each participant, we acquired a reference echoplanar imaging scan, which we visually inspected for artifacts (e.g. ghosting) and good signal across the entire volume of acquisition, including the amygdala and ventral striatum. Additionally, an autoshimming procedure was conducted before the acquisition of BOLD data in each participant to minimize field inhomogeneities. The fMRI data from all participants included in this study were free of such problems.

BOLD fMRI Data Analysis

Whole-brain image analysis was completed using the general linear model of SPM2 (Wellcome Department of Imaging Neuroscience, London, England). Images for each participant were realigned to the first volume in the time series to correct for head motion, spatially normalized into a standard stereotactic space (Montreal Neurological Institute template) using a 12-parameter affine model, and smoothed to minimize noise and residual difference in gyral anatomy with a Gaussian filter set at 6 mm full-width at half-maximum. Voxel-wise signal intensities were ratio-normalized to the whole-brain global mean.

After preprocessing, linear contrasts using canonical hemodynamic response functions were used to estimate condition-specific (i.e. Faces > Shapes) BOLD activation for each individual. These individual contrast images (i.e. weighted sum of the beta images) were then used in second-level random-effects models to create a group map of the main effect of task on amygdala activation. Our amygdala region of interest was constructed using the Talairach Daemon option of the WFU PickAtlas Tool, version 1.04 (Wake Forest University School of Medicine, Winston-Salem, NC). Individual BOLD values from the functional amygdala clusters were extracted using the VOI tool in SPM2. Analyses involving ADCY7 genotype were conducted using these values outside of SPM thereby eliminating any possibility of correlations that are artificially inflated due to extraction and correlation techniques that capitalize on the same data twice (20). In sum, our analytic method was quite conservative and yet still demonstrated robust effects across samples.

Table S1. Altered gene expression in SERT^{KO} mice. See Supplement 2 (Excel file) for this table. alr, average log-ratio; avg, average; AMY, amygdala; CC, cingulate cortex; FC, functional connectivity; KO, knock-out; WT, wild-type.

Table S2. Mouse-Human altered gene expression.

Gene	Gene Symbol	Mouse (alr)	p-value	Human (alr)	p-value
Amygdala					
adenylate cyclase 7	<i>ADCY7</i>	0.60	0.04	0.40	0.02
voltage-dependent calcium channel	<i>CACNA1D</i>	0.33	0.02	0.41	0.03
potassium channel-interacting protein 4	<i>KCNIP4</i>	0.43	0.02	0.48	0.02
lin-7 homolog	<i>LIN7C</i>	0.48	0.05	0.31	0.01
nuclear receptor 1D2	<i>NR1D2</i>	0.45	0.01	0.47	0.04
potassium channel tetramerisation domain	<i>KCTD9</i>	0.17	0.04	0.55	0.03
mitogen-activating protein kinase kinase 2	<i>MAP2K2</i>	-0.42	<.005	-0.32	0.02
amyloid beta (A4) precursor-like protein 2	<i>APLP2</i>	0.47	0.01	0.45	0.03
ankyrin repeat domain 6	<i>ANKRD6</i>	0.46	0.03	0.42	0.02
calcium activated nucleotidase 1	<i>CANT1</i>	0.45	0.02	0.22	0.01
choline phosphotransferase 1	<i>CHPT1</i>	0.28	0.02	0.56	0.04
coiled-coil domain containing 50	<i>CCDC50</i>	0.32	0.03	0.33	0.03
coxsackie virus and adenovirus receptor	<i>CXADR</i>	0.27	0.02	0.27	0.02
fibroblast growth factor	<i>FGF14</i>	0.52	<0.005	0.56	<0.005
golgi SNAP receptor complex member 1	<i>GOSR1</i>	0.47	<0.005	0.37	0.01
nucleoporin 50	<i>NUP50</i>	0.36	<0.005	0.36	0.02
nucleoporin-like 1	<i>NUPL1</i>	0.31	0.05	0.13	0.04
PBX/knotted 1 homeobox	<i>PKNOX1</i>	0.44	0.01	0.38	0.04
pleckstrin homology domain	<i>PLEKHF2</i>	0.38	0.04	0.59	0.01
Ras-like without CAAX 2	<i>RIT2</i>	0.31	0.03	0.48	0.04
ribonucleotide reductase M1	<i>RRM1</i>	0.27	<.005	0.64	0.03
ring finger protein 170	<i>RNF170</i>	0.28	0.03	0.32	0.04
solute carrier family 25	<i>SLC25A27</i>	0.28	0.04	0.30	0.02
sulfiredoxin 1 homolog	<i>SRXN1</i>	0.31	0.01	0.30	0.02
TBC1 domain family 4	<i>TBC1D4</i>	0.63	0.04	0.25	0.01
WD repeat domain 1	<i>WDR1</i>	0.26	0.04	0.49	0.01
TAF15 RNA polymerase II	<i>TAF15</i>	-1.42	<0.005	-0.30	0.03
zinc finger protein 444	<i>ZFP444</i>	-0.44	0.03	-0.36	0.02
Cingulate					
aminoadipate-semialdehyde dehydrogenase-phosphopantetheinyl transporter	<i>AASDHPPT</i>	0.88	0.005	0.34	0.002
CCAAT/enhancer binding protein	<i>CEBPG</i>	0.39	0.048	0.21	0.01
E1A binding protein p300	<i>EP300</i>	0.29	0.014	0.27	0.037
EPH receptor A5	<i>EPHA5</i>	0.50	<.0005	0.21	0.027
protein phosphatase 1A	<i>PPM1A</i>	0.54	0.008	0.28	0.013
Rho GTPase activating protein 5	<i>ARHGAP5</i>	0.52	0.036	0.24	0.01
sorting nexin 13	<i>SNX13</i>	0.35	0.042	0.34	0.018

arestin domain containing 3	<i>ARRDC3</i>	0.46	0.034	0.36	0.035
coproporphyrinogen oxidase	<i>CPOX</i>	0.57	0.008	0.27	0.013
fucose-1-phosphate guanylyltransferase	<i>FPGT</i>	0.46	0.029	0.33	0.029
metal response element binding transcription factor 2	<i>MTF2</i>	0.69	0.013	0.26	0.039
protein-L-isoaspartate O-methyltransferase domain	<i>PCMTD1</i>	0.45	0.009	0.35	<0.0005
sperm associated antigen 9	<i>SPAG9</i>	0.38	0.032	0.28	0.005
splicing factor proline/glutamine rich transmembrane and tetratricopeptide repeat containing 2	<i>SFPQ</i>	0.32	0.011	0.27	<.0005
transmembrane protein 64	<i>TMEM64</i>	0.57	0.013	0.37	0.025
Yip1 domain 5	<i>YIPF5</i>	0.44	0.005	0.26	0.025
PDZ domain 4	<i>PDZD4</i>	-0.3	0.034	-0.32	0.018

alr, average log-ratio.

Supplemental References

1. Holmes A, Murphy DL, Crawley JN (2003): Abnormal behavioral phenotypes of serotonin transporter knockout mice: parallels with human anxiety and depression. *Biol Psychiatry* 54:953-9.
2. Lira A, Zhou M, Castanon N, Ansorge MS, Gordon JA, Francis JH, *et al.* (2003): Altered depression-related behaviors and functional changes in the dorsal raphe nucleus of serotonin transporter deficient mice. *Biol Psychiatry* 54(10):960-71.
3. Murphy DL, Lesch KP (2008): Targeting the murine serotonin transporter: insights into human neurobiology. *Nat Rev Neurosci* 9:85-96.
4. Joeyen-Waldorf J, Edgar N, Sibille E (2009): The roles of sex and serotonin transporter levels in age- and stress-related emotionality in mice. *Brain Res* 1286:84-93.
5. Ansorge MS, Zhou M, Lira A, Hen R, Gingrich JA (2004): Early-life blockade of the 5-HT transporter alters emotional behavior in adult mice. *Science* 306:879-81.
6. Santarelli L, Saxe M, Gross C, Surget A, Battaglia F, Dulawa S, *et al.* (2003): Requirement of hippocampal neurogenesis for the behavioral effects of antidepressants. *Science* 301:805-9.
7. Bengel D, Murphy DL, Andrews AM, Wichems CH, Feltner D, Heils A, *et al.* (1998): Altered brain serotonin homeostasis and locomotor insensitivity to 3, 4-methylenedioxymethamphetamine ("Ecstasy") in serotonin transporter-deficient mice. *Mol Pharmacol* 53:649-55.
8. Sibille E, Pavlides C, Benke D, Toth M (2000): Genetic inactivation of the Serotonin(1A) receptor in mice results in downregulation of major GABA(A) receptor alpha subunits, reduction of GABA(A) receptor binding, and benzodiazepine-resistant anxiety. *J Neurosci* 20:2758-65.

9. Bodnoff SR, Suranyi-Cadotte B, Aitken DH, Quirion R, Meaney MJ (1988): The effects of chronic antidepressant treatment in an animal model of anxiety. *Psychopharmacology (Berl)* 95:298-302.
10. Sibille E, Wang Y, Joeyen-Waldorf J, Gaiteri C, Surget A, Oh S, *et al.* (2009): A molecular signature of depression in the amygdala. *Am J Psychiatry* 166:1011-1024.
11. Pronko SP, Saba LM, Hoffman PL, Tabakoff B (2010): Type 7 adenylyl cyclase-mediated hypothalamic-pituitary-adrenal axis responsiveness: influence of ethanol and sex. *J Pharmacol Exp Ther* 334:44-52.
12. First MB, Spitzer RL, Gibbon M, Williams JBM (1996): *Structured Clinical Interview for DSM-IV Axis I Disorders, Research Version, Non-patient Edition*. New York State Psychiatric Institute, Biometrics Research Department: New York, NY.
13. Brown SM, Peet E, Manuck SB, Williamson DE, Dahl RE, Ferrell RE, Hariri AR (2005): A regulatory variant of the human tryptophan hydroxylase-2 gene biases amygdala reactivity. *Mol Psychiatry* 10:884-8.
14. Brown SM, Manuck SB, Flory JD, Hariri AR (2006): Neural basis of individual differences in impulsivity: contributions of corticolimbic circuits for behavioral arousal and control. *Emotion* 6:239-45.
15. Manuck SB, Brown SM, Forbes EE, Hariri AR (2007): Temporal stability of individual differences in amygdala reactivity. *Am J Psychiatry* 164:1613-4.
16. Darwin C, Ekman P (1998): *The Expression of the Emotions in Man and Animals*. 3rd ed. Oxford University Press: New York, NY.
17. Ekman P, Friesen W (1976): *Pictures of Facial Affect*. Consulting Psychologists Press: Palo Alto, CA.
18. Schwartz CE, Wright CI, Shin LM, Kagan J, Rauch SL (2003): Inhibited and uninhibited infants "grown up": adult amygdalar response to novelty. *Science* 300:1952-3.

19. Wright CI, Martis B, Schwartz CE, Shin LM, Fischer H H, McMullin K, Rauch SL (2003): Novelty responses and differential effects of order in the amygdala, substantia innominata, and inferior temporal cortex. *Neuroimage* 18:660-9.
20. Viviani R (2010): Unbiased ROI selection in neuroimaging studies of individual differences. *Neuroimage* 50:184-9.